Variation in carotenoid–protein interaction in bird feathers produces novel plumage coloration

Maria M. Mendes-Pinto[1], Amy M. LaFountain[2], Mary Caswell Stoddard[5], Richard O. Prum[3,4], Harry A. Frank[2],* and Bruno Robert[1],*

[1]*Institut de Biologie et de Technologie de Saclay, CEA, URA 2096 CNRS, CEA Saclay 91191 Gif sur Yvette, France*
[2]*Department of Chemistry, University of Connecticut, 55 North Eagleville Road, Storrs, CT 06269, USA*
[3]*Department of Ecology and Evolutionary Biology and Peabody Museum of Natural History, Yale University, 21 Sachem Street, New Haven, CT 06511, USA*
[4]*Donostia International Physics Center (DIPC), Paseo Manuel de Lardizabal 3, 20018 Donostia-San Sebastian, Spain*
[5]*Department of Zoology, University of Cambridge, Downing Street, Cambridge CB2 3EJ, UK*

Light absorption by carotenoids is known to vary substantially with the shape or conformation of the pigment molecule induced by the molecular environment, but the role of interactions between carotenoid pigments and the proteins to which they are bound, and the resulting impact on organismal coloration, remain unclear. Here, we present a spectroscopic investigation of feathers from the brilliant red scarlet ibis (*Eudocimus ruber,* Threskiornithidae), the orange-red summer tanager (*Piranga rubra,* Cardinalidae) and the violet-purple feathers of the white-browed purpletuft (*Iodopleura isabellae,* Tityridae). Despite their striking differences in colour, all three of these feathers contain canthaxanthin (β,β-carotene-4,4′-dione) as their primary pigment. Reflectance and resonance Raman (rR) spectroscopy were used to investigate the induced molecular structural changes and carotenoid–protein interactions responsible for the different coloration in these plumage samples. The results demonstrate a significant variation between species in the peak frequency of the strong ethylenic vibration (ν_1) peak in the rR spectra, the most significant of which is found in *I. isabellae* feathers and is correlated with a red-shift in canthaxanthin absorption that results in violet reflectance. Neither polarizability of the protein environment nor planarization of the molecule upon binding can entirely account for the full extent of the colour shift. Therefore, we suggest that head-to-tail molecular alignment (i.e. J-aggregation) of the protein-bound carotenoid molecules is an additional factor.

Keywords: absorption spectroscopy carotenoid; coloration; β-keratin; electronic transition; resonance Raman spectroscopy

1. INTRODUCTION

Carotenoid pigments contribute to colour of feathers and are thought to be important for communication in many bird species [1–5]. Coloration in feathers can arise from light scattering by nanostructures, or from the presence of pigments that absorb light in particular regions of the electromagnetic spectrum [2,6,7]. Nanostructures usually produce UV-to-turquoise, white or iridescent colours [6,8]. Melanins are associated with black and browns [6,7,9]. Carotenoids give rise to yellow, orange and red coloration [2]. Green colours in feathers often results from a combination of yellow pigmentation and blue structural colours [6,10,11]. All of these factors contribute to make bird feather coloration as one of the most striking displays in all of nature.

Birds do not synthesize carotenoids de novo, and therefore must ingest them along with their diet [2,12,13]. After ingestion, carotenoids are transported to various body tissues where they accumulate and carry out their biological roles [2,13]. Common carotenoids in bird diets are β-carotene, lutein, zeaxanthin and β-cryptoxanthin [13–16]. Coloration in feathers may arise directly from deposition of dietary carotenoids [2,17]. Alternatively, ingested carotenoids may be metabolically modified before deposition, for example, by ketolase activity at the β- and ε-rings [2,18,19].

Figure 1. Plumages coloration of the (*a*) scarlet ibis *Eudocimus ruber* (Threskiornithidae, image courtesy of G. Armistead/ VIREO), (*b*) the male summer tanager *Piranga rubra* (Cardinalidae, image courtesy of R. Nussbaumer/VIREO) and (*c*) the white-browed purpletuft *Iodopleura isabellae* (Tityridae, photograph courtesy of Nick Athanas).

It is known that carotenoids incorporated during feather development bind strongly to proteins in the structures [11,13,20]. The proteins have a heterogeneous amino acid composition that can vary even in the same feather, depending on the required physical properties [21,22]. Owing to different pigment–protein interactions, the same carotenoid composition can give rise to different colours in feathers from various species or to different coloured patches of feathers in the same species [11,20]. A similar phenomenon has been observed for the coloration of exoskeletons of crustaceans [11,20,23–27].

Resonance Raman (rR) spectroscopy provides direct, selective information regarding the structure of the electronic ground state of carotenoid molecules [28–30]. By matching the energy of incident light with the energy of the electronic absorption of a given carotenoid, selective probing of a subpopulation of molecules in a complex mixture may be achieved [28,31], thus allowing structural characterizations *in situ*. rR spectra of carotenoids are characterized by four distinct bands denoted ν_1 through ν_4, whose frequencies vary with the effective conjugation length of the π-electron double bond chain in the molecule, geometric isomeric configuration and degree of distortion [27,29,30,32]. In an analysis of yellow and red-coloured patches of the European goldfinch (*Carduelis carduelis*), which are pigmented by canary xanthophylls (ε,ε-carotene-3,3′-dione and 3′-hydroxy-ε,ε-caroten-3-one), Stradi *et al.* [11] documented variation in the energy of the strongly allowed $S_0 \rightarrow S_2$ electronic transition by rR spectroscopy. This variation was due to an apparent change in the bond alternation of the conjugated polyene chain of the protein-bound carotenoids, suggesting an influence of the molecular environment on the binding of the pigments [11].

In *C. carduelis*, the effect of feather protein binding was to shift the colour from yellow to red—two plumage colours that are also easily produced independently by changes in carotenoid molecular structure. So, it is not clear that association with the protein can contribute to novel plumage colours. In the present study, we employed rR spectroscopy to investigate carotenoid–protein interactions responsible for the coloration of brilliant red and purple plumages of the scarlet ibis *Eudocimus ruber* (Threskiornithidae), summer tanager *Piranga rubra* (Cardinalidae) and white-browed purpletuft *Iodopleura isabellae* (Tityridae). All these plumage patches contain canthaxanthin (β,β-carotene-4,4′-dione) as the primary carotenoid [33–35] (figure 1).

The violet colour of male *I. isabellae* is very rare in bird plumages, and nothing is known about its production in *Iodopleura*.

In this study, rR and absorption spectra deduced from reflectance spectra of canthaxanthin bound *in situ* were compared with those recorded from canthaxanthin in solution to evaluate the molecular basis for the different spectral shifts that result in distinct colours of the feathers. We predict that the spectral differences of these three birds can be attributed to novel modes of binding canthaxanthin within the keratin matrix of the feathers, and postulate the involvement of specific factors including polarizability of the molecular environment and binding-induced configurational changes (e.g. planarization of the terminal rings). It should be noted that the nature of the bond between the carotenoid pigment and the specific structural component of the feather was not explored herein, and while it is possible that the pigment could bind to lipid components of the feather, it is generally accepted that carotenoids are bound directly to keratin or to other proteins in the feather [11,20]. The characterization of the molecular factors responsible for these differences will further elucidate how birds have evolved to use variation in the molecular environment of pigment binding to tune the electronic properties of specific carotenoid molecules.

2. MATERIAL AND METHODS

2.1. Extraction and analysis of carotenoids

Red back feathers of a male *E. ruber* (YPM 26570; collected March 1951), red–orange belly feathers of a male *P. rubra* (YPM 7362, collected June 1957; YPM 3771, no collection data) and feathers from the purple pectoral tufts of a male *I. isabellae* (YPM 77812, no collection data; AMNH 494716, collected in 1886) were obtained from the Yale Peabody Museum of Natural History, Yale University, New Haven, CT, USA and the American Museum of Natural History, New York, NY, USA. Specimens were chosen for the high quality of colour preservation based on visual evaluation by R.O.P.

All-trans-canthaxanthin (β,β-carotene-4,4′-dione) was obtained from Roche. Carotenoids were extracted from the feathers, as previously described by LaFountain *et al.* [36]. An HPLC analysis was conducted using a Waters 600E multi-solvent delivery system with an

in-line Waters 2996 photodiode array detector and a Phenomenex Luna 5 μm silica column (250 × 4.6 mm). The mobile phase consisted of a linear gradient from 90 : 10 to 80 : 20 hexanes/acetone (Fisher Scientific, Pittsburgh, PA, USA) over a period of 40 min, with a flow rate of 1.5 ml min^{-1}. The injection solvent was 14 per cent acetone and 86 per cent hexanes. The details of the mass spectrometry analysis can be found in the electronic supplementary material, figure S1.

2.2. Spectroscopy

Reflectance spectra of the feathers were measured using procedures previously described [37]. Briefly, the measurements were carried using an Ocean Optics S2000 spectrometer with an Ocean Optics DH-2000-BAL deuterium–halogen light source. Measurements were integrated for 500 ms at a distance of approximately 6 mm from the plumage with a perpendicular incident light, resulting in a approximately 3 mm^2 illumination field. The probe was secured in an aluminium block to obscure ambient light. The following formula was used to calculate per cent reflectance (%R):

$$\%R = \left[\frac{S - D}{W - D} \right] \times 100,$$

where S is the reflectance of the specimen, D is the reflectance of the dark standard and W is the reflectance of the white standard. The white standard was determined by measuring the reflectance of a white Spectralon tablet from Ocean Optics, while the dark standard was measured using ambient light in a darkened room [37].

Absorption spectra of *all-trans*-canthaxanthin in methanol, acetonitrile, tetrahydrofuran, hexane, diethylether, cyclohexane, toluene and carbon disulphide (all purchased from Sigma-Aldrich, St. Louis, MO, USA) were recorded at room temperature, using a Varian Cary E5 double-beam scanning spectrophotometer. These solvents were chosen to represent a wide range of polarizabilities. rR spectra of canthaxanthin were obtained in hexane and diethylether at room temperature, using a Jobin-Yvon U1000 rR spectrophotometer equipped with a front-illuminated, deep-depleted CCD detector (Synapse Horiba, Jobin Yvon, France). Excitation at 457.9, 488, 514.5 and 528.7 nm was provided by a Sabre argon ion laser (Coherent, Palo Alto, CA, USA) and at 568.2 nm by an Innova 90 krypton ion laser (Coherent). For *in situ* rR spectroscopic experiments, a confocal microscope Olympus BX41 was coupled to the spectrometer. The same slit-width (200 μm) and grating were used for both systems, thereby achieving the same spectral resolution. The excitation beam was defocused and kept at a sufficiently low power (typically less than 20 mW) to prevent degradation of the sample by the absorbed light energy. Systematic comparison of rR spectra was performed throughout the time duration of each experiment to confirm sample integrity.

2.3. Avian colour space modelling

Avian perception of colour was modelled using a tetrahedral colour space [3,37], which provides a quantitative representation of sensory experience, using the computer program TETRACOLORSPACE v. 1. 0 for MATLAB 7 [3,37] (available for free from the authors). The idealized stimulus, Q_I, of each single cone type was estimated by the reflectance spectrum of a plumage patch:

$$Q_I = \int_{300}^{700} R(\lambda) C_r(\lambda) \mathrm{d}\lambda, \qquad (2.1)$$

where $R(\lambda)$ is the reflectance spectrum of the plumage patch, and $C_r(\lambda)$ is the spectral sensitivity function of each cone type r. For each plumage colour, the idealized stimulation values of the four single cones—Q_I—were normalized to sum to one, yielding relative $[uv/v \ s \ m \ l]$ values. The $[uv/v \ s \ m \ l]$ values were converted to a colour point with spherical coordinates θ, ϕ and r, which define a colour vector pointing from the achromatic point is at the origin. Hue is the direction of the vector, given by the angles θ and ϕ, and saturation is the length of the vector, r [3,37].

We modelled *E. ruber*, *P. rubra* and *I. isabellae* reflectance spectra in avian tetrahedral colour space using a standard violet cone-type visual system [38], which is the ancestral condition in birds [39,40]. We further compared the colour space distribution of *E. ruber*, *P. rubra* and *I. isabellae* reflectance spectra to a diverse sample of avian orders and families (including data from Stoddard & Prum [3] on all non-cotinga species having plumage coloration either inferred or identified as carotenoid-based).

3. RESULTS

Both the feather reflectance spectra (figure 2a) and the inferred absorption, spectra (figure 2b) are broad and relatively structureless, which is typical of keto-carotenoids [41]. The absorption spectra of the feathers from *E. ruber* and *P. rubra* are very similar, and have an absorption maximum (reflectance minimum) centred at 495 nm. However, the absorption spectra of *E. ruber* feathers are much broader than *P. rubra*, resulting in a substantially redder reflectance and the near elimination of the *P. rubra* reflectance peak in the near ultraviolet at 361 nm. The spectra of the purple feathers of *I. isabellae* display a maximum absorbance (minimum reflectance) shifted to longer wavelengths, peaking at approximately 570 nm. Consequently, the high-energy reflectance peak of *I. isabellae* is shifted well into the human visible spectrum, resulting in a blue reflectance peak at 426 nm. Combined with the long-wavelength reflectance above 600 nm (on from the far side of the 570 nm absorbance peak), the blue and red reflectance create an entirely pigmentary violet colour.

An HPLC analysis of the carotenoids extracted from feathers of *E. ruber*, *P. rubra*, and *I. isabellae* demonstrated the presence of a single major carotenoid in all three samples (figure 3). On the basis of its absorption spectra and retention times, the carotenoid was unambiguously identified as *all-trans*-canthaxanthin (β,β-carotene-4,4′-dione) (figure 3). This identification was confirmed by mass spectrometry (see electronic supplementary material, figure S1) as well as by the HPLC of a heated bona fide canthaxanthin standard
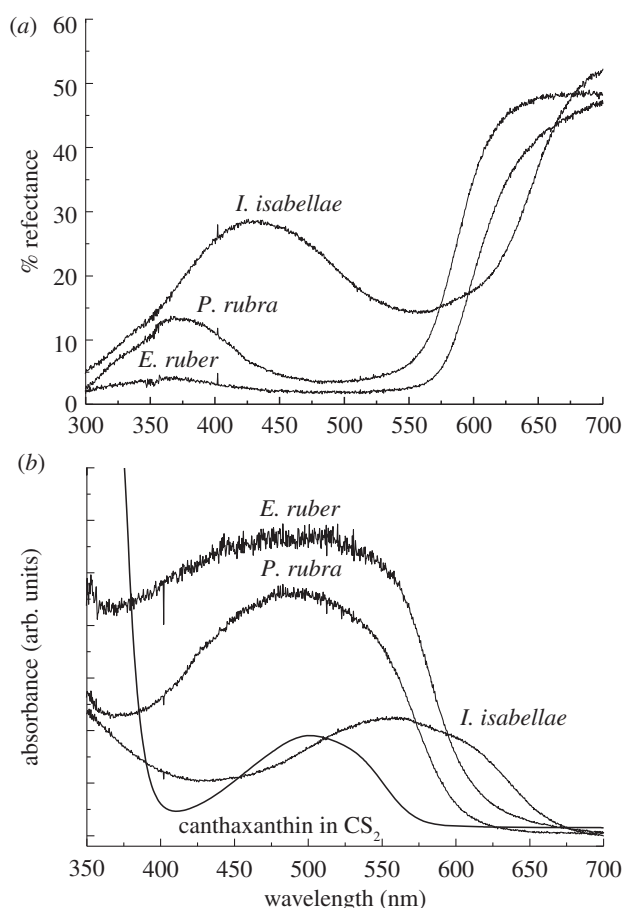
Figure 2. (*a*) Single reflectance spectra of the red back feathers of *E. ruber* (YPM 26570), the red–orange belly feathers of a male *P. rubra* (YPM 7362) and the purple breast feathers of male *I. isabellae* (YPM 77812); (*b*) Optical absorption spectra of the feathers computed from the reflectance spectra using $A = -\log(R)$, where R = reflectance.

run under the same conditions (figure 3*d*). This sample also demonstrated that the smaller peaks eluting in proximity to the major peaks are associated with *cis*-canthaxanthin formed during the heating and extraction process. The absorption spectrum of *cis*-canthaxanthin is confirmed by a slight blue-shift in the absorption spectrum relative to that of *all-trans*-canthaxanthin and the large *cis*-band appearing at approximately 360 nm (dashed traces in figure 3). These findings confirm previous reports that canthaxanthin is the primary pigment of *E. ruber* and *P. rubra* [33–35]. While canthaxanthin was found to be the dominant pigment in all three birds, *E. ruber* and *P. rubra* were also found to contain small amounts of other carotenoids. A pigment isolated from *E. ruber* with a retention time of 5.0 min displayed a blue-shifted absorption spectrum suggestive of a shortened conjugated chain (figure 3*c*). This pigment was found to have a mass of 568 m/z, which is consistent with bis-dihydrocanthaxanthin, a carotenoid previously reported in *E. ruber* plumage by Fox & Hopkins [33]. *Piranga rubra* plumage was found to contain a minor pigment that eluted at 9.7 min and had a featureless absorption spectrum consistent with a keto-carotenoid, and a mass of 580 m/z. Additional small peaks were observed in the HPLC chromatograms of these two

birds; however, further analysis of these pigments was precluded owing to a lack of material. Some of the minor peaks in each chromatogram could be attributed to *cis*-isomers of canthaxanthin that were formed during the extraction procedure.

Saranathan *et al.* [42] have used small-angle X-ray scattering (SAXS) to assay the nanoscale variation in refractive index in structurally coloured and pigmented feathers. Unlike structurally coloured feathers with spongy β-keratin nanostructures [43–46], the azimuthal average of the SAXS data from *I. isabellae* shows no peaks for any optically relevant spatial frequencies, or *q*-values (see electronic supplementary material, figure S2). Rather, the azimuthal average has a slope that is closely congruent to Porod's Law (q^{-4}), the expectation for a random heterogeneous mixture of two materials with well-defined interface [47]. In the absence of any nanostructure that could enhance the coherent scattering of blue light, the purple feathers of male *I. isabellae* are produced by pigmentary absorption.

The absorption spectrum of canthaxanthin in solution exhibits only small modulations within the spectrum, and appears as a single, broad band (see the spectrum of canthaxanthin in CS_2, figure 2*b*). This type of broad band corresponds to the strongly allowed $S_0 \rightarrow S_2$ electronic transition, which gives carotenoids their characteristic visible coloration [48]. The position of the spectral origin (0–0) of the $S_0 \rightarrow S_2$ transition can be determined from the longest-wavelength minimum of the second derivative of the absorption spectrum. The energy of this (0–0) band in solution depends primarily on the refractive index, *n*, of the solvent, and there is a small influence of the solvent dielectric constant [49]. As n increases, the polarizability, $R(n)$, of the solvent expressed as $R(n) = (n^2-1)/(n^2+2)$ also increases, and the position of the $S_0 \rightarrow S_2$ transition shifts to longer wavelength. In the present work, we evaluated the effect of solvent polarizability on the position of the (0–0) spectral origin band of the $S_0 \rightarrow S_2$ electronic transition of canthaxanthin in solution (figure 4). The spectral origin varies linearly over approximately 40 nm for a variety of solvents with a wide range of $R(n)$ (figure 4).

Room temperature rR spectra of canthaxanthin dissolved in hexane and diethylether contain the four main groups of bands, denoted ν_1 through ν_4, that are typical of carotenoid molecules (figure 5) [30,32]. The ν_1 band around 1520 cm^{-1} arises from stretching vibrations of C=C double bonds, and its frequency depends on both the length of the π-electron conjugated chain of the carotenoid and its configuration; i.e. the extent and position of twisting along the carbon backbone of the molecule [29,50,51]. The ν_2 band around 1160 cm^{-1} is due mainly to stretching vibrations of C–C single bonds coupled with C–H in-plane bending modes [29,32]. The rR bands in the vicinity of ν_2 are also sensitive to the position of twisting along the carbon backbone and this constitutes the 'fingerprint region' for the assignment of carotenoid configurations [50]. The ν_3 band at approximately 1010 cm^{-1} arises from the coupling of the in-plane rocking vibration of the methyl groups attached to the conjugated chain with the adjacent C–H in-plane bending modes
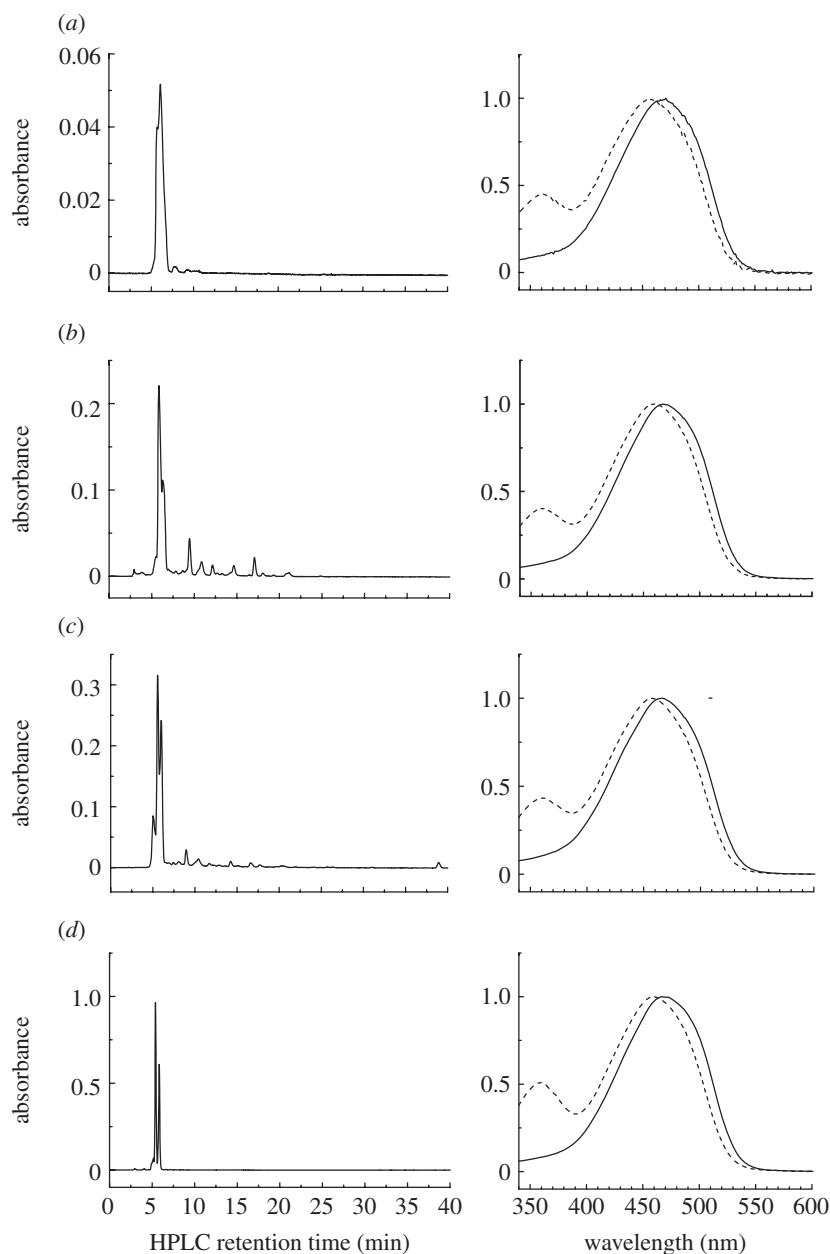
Figure 3. Normal-phase HPLC chromatogram of the extracts from feathers of *E. ruber*, *P. rubra* and *I. isabellae* carried out as described in the text. The chromatograms were detected at 470 nm. (*a*) *I. isabellae*: solid line, 5.7 min; dashed line, 6.6 min; (*b*) *P. rubra*: solid line, 5.8 min; dashed line, 6.3 min; (*c*) *E. ruber*: solid line, 5.6 min; dashed line, 6.0 min; (*d*) heated canthaxanthin solid line, 5.7 min; dashed line, 6.6 min.

[30,32]. The ν_4 band around 960 cm^{-1} arises from C–H out-of-plane wagging motions coupled with C=C torsional modes that are out-of-plane twists of the carbon backbone [30,32]. If the π-electron conjugated system in the carotenoid is symmetric, as it is in canthaxanthin, the out-of-plane ν_4 modes will not be coupled with the electronic transition when the molecule is planar. Accordingly, these bands will not be resonance-enhanced upon excitation and will exhibit very low intensity in the rR spectra. However, they will increase in intensity when distortions around C–C single bonds occur [52]. For canthaxanthin in solution (figure 5), the ν_4 band exhibits two weak overlapping components between 955 and 964 cm^{-1}. This result indicates that the average relaxed state of canthaxanthin in solution corresponds to a geometry

deviating slightly from completely planar. An X-ray structure analysis of crystalline canthaxanthin supports the view that the terminal rings in the molecule are asymmetrically twisted out of the plane of the conjugated π-electron C=C chain by approximately 55° [53].

The rR spectra of *E. ruber*, *P. rubra* and *I. isabellae* were measured by rR microspectroscopy using excitation wavelengths of 457.9, 488, 514.5, 528.7 and 568.2 nm, which span the carotenoid absorption transition (figure 6). For *P. rubra* feathers (figure 6*a*), the rR spectra are not dependent on the excitation wavelength and resemble that of *all-trans*-canthaxanthin in solution. The ν_1 band is positioned at precisely 1514.3 cm^{-1} for all excitation wavelengths (table 1), but its full-width at half-maximum (fwhm) is 21.4 cm^{-1} for excitation at 457.9 nm compared with 21.6 cm^{-1} at 514.5 nm, which
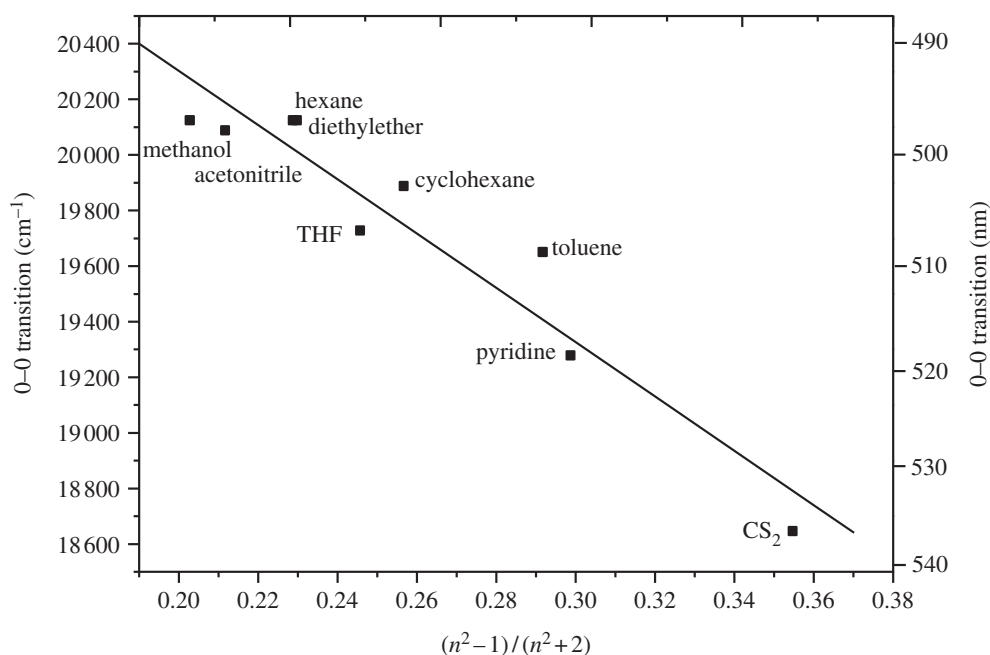
Figure 4. Position of the (0–0) bands of the $S_0 \rightarrow S_2$ electronic transition of canthaxanthin as a function of polarizability in different solvents.
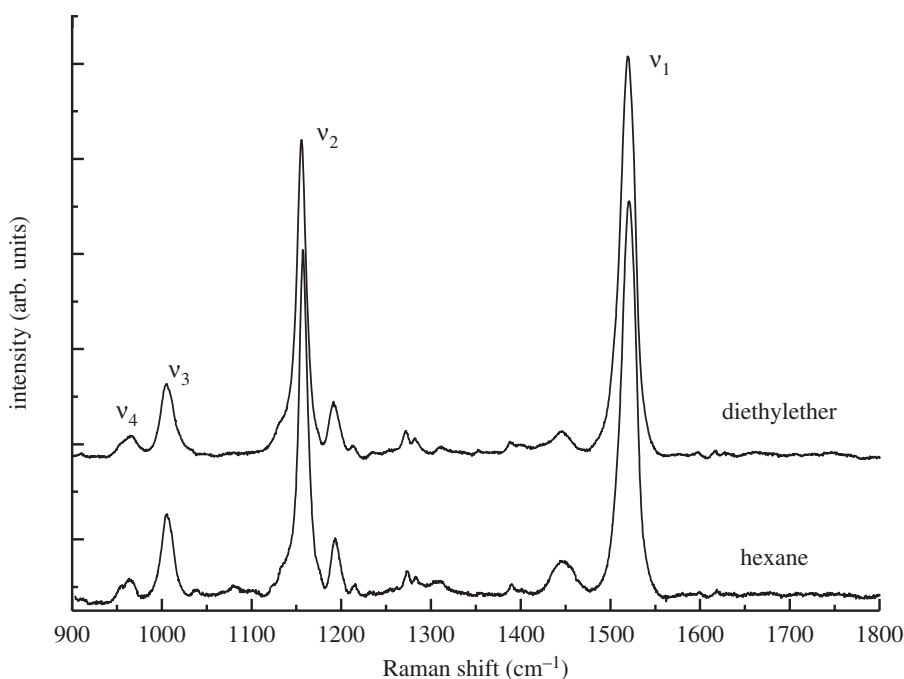

Figure 5. Room temperature rR spectra of canthaxanthin in diethylether and hexane. Excitation wavelength, 514.5 nm. Four distinct bands denoted ν_1 to ν_4 are observed in the spectra whose frequencies vary as described in the text.

is suggestive of a slight variation in carotenoid binding. However, the spectra indicate little out-of plane distortion upon binding canthaxanthin to the protein. From a structural point of view, the strong similarity in the spectra taken using the different excitation wavelengths are suggestive of a single pool of *all-trans*-canthaxanthin molecules in these feathers. Thus, little difference in canthaxanthin absorption is predicted between *P. rubra* and canthaxanthin in solution except for the widening of the absorbance owing to slight variation shown by the width of ν_1.

The rR spectra of *E. ruber* feathers (figure 6b) are typical of *all-trans*-canthaxanthin, but the frequency of the ν_1 band varies between 1512.1 and 1519.7 cm^{-1}, depending on the excitation wavelength. In addition, the fwhm of the ν_1 band is 3 cm^{-1} larger than observed for *P. rubra*. The fwhm of the ν_1 band is largest (approx. 28 cm^{-1}) when the shortest wavelength (457.9 nm) excitation is used. This is suggestive of a heterogeneous population of twisted, but not fully isomerized, *all-trans*-canthaxanthin molecules in *E. ruber* feathers. These results are consistent with the reflectance and
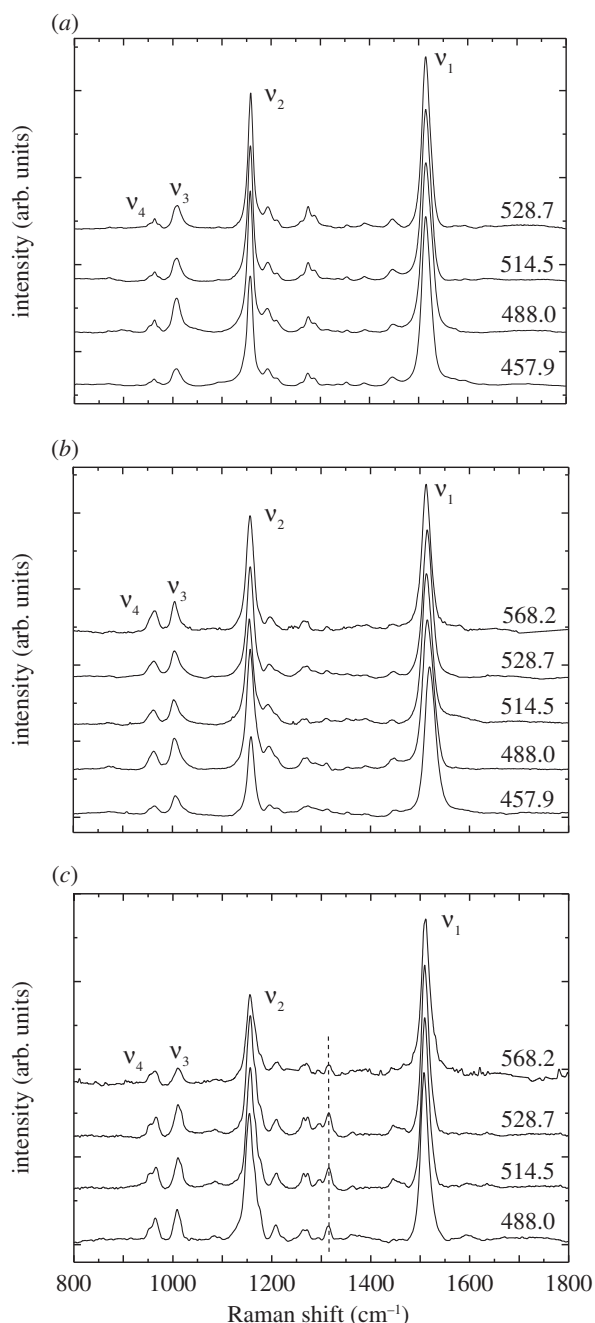
Figure 6. rR spectra of the feathers from: (*a*) *P. rubra;* (*b*) *E. ruber* and (*c*) *I. isabellae.* The excitation wavelengths in nm units are indicated on the right-hand side of the figure. The peak at approximately 1317 cm^{-1} in figure 6*c* is not associated with a carotenoid (dashed line).

absorption spectra obtained from these feathers (figure 2), which show that the electronic absorption transition of *E. ruber* feathers is even broader than that observed from *P. rubra*. In *E. ruber* feathers, the overall intensity in the ν_4 band region compared with that of the ν_3 bands is higher than for *P. rubra* feathers. This is particularly true for excitation wavelengths longer than 488.0 nm and indicates distortion of the relaxed geometric state of canthaxanthin in the feathers from *E. ruber*.

Resonance rR spectra of *I. isabellae* feathers recorded using different excitation wavelengths were very similar

(figure 6*c*), indicating the presence of a single pool *all-trans*-canthaxanthin molecules with some differences in the frequencies compared with the spectra taken from the other feathers and from canthaxanthin in solution. The frequency of the ν_1 band, which occurs between 1507.5 and 1509.6 cm^{-1}, is substantially lower than that observed in the feathers from the other two species and from canthaxanthin in solution (figures 5 and 6; table 1). The frequency of the ν_1 band is approximately 7 cm^{-1} lower than the ν_1 peak from *P. rubra* and *E. ruber* (at an excitation wavelength of 488 nm) and up to 12.5 cm^{-1} lower than the ν_1 peak of canthaxanthin in solution. Given that ν_1 is associated with the stretching of C=C double bonds [29,50], this result is associated with a physical extension of the effective **π**-electron conjugated chain within the molecular backbone of canthaxanthin in *I. isabellae*, which is functionally correlated with the observed red-shift in its absorbance.

Also, the structure of the ν_2 band in *I. isabellae* is rather unusual for carotenoid molecules in organisms. Typically, the satellite bands associated with the intense band at approximately 1160 cm^{-1} appear as two distinct bands (see e.g. spectra of lutein in the work by Ruban *et al.* [54]). This is also the case for the feathers from *P. rubra* and *E. ruber* (figure 6*a,b*, respectively). For *I. isabellae*, the ν_2 band at approximately 1155 cm^{-1} displays only one satellite band at 1209 cm^{-1}. Purified canthaxanthin in solution also exhibits only one satellite band in that region, however at a lower frequency (approx. 1190 cm^{-1}; figure 5). Lastly, the ν_4 band in the rR spectra from *I. isabellae* feathers (figure 6*c*) has a significantly high intensity compared with that seen from canthaxanthin in solution (figure 5). This result is indicative of molecular distortion.

To examine further the effect of variation in carotenoid binding on the colours that birds perceive, we compared the reflectance spectra of *E. ruber*, *P. rubra* and *I. isabellae* to the entire gamut of avian carotenoid plumages using a tetrachromatic model of avian colour vision [3,37]. Because birds have four single cones—red, green blue and violet/ultraviolet—their colour perceptions can be modelled with a tetrahedral colour space, or simplex [3,55]. In figure 7, we show the total diversity of colour perceptions produced by carotenoid plumages of more than 50 species in 23 avian families (gray circles and polyhedron, figure 7). Using canthaxanthin pigment only, the plumage colours of *E. ruber* (red dots), *P. rubra* (orange dots) and *I. isabellae* (purple dot) span a huge range of the carotenoid plumage gamut. Using canthaxanthin pigments, the maximum span (the distance between *E. ruber* and *I. isabellae*) is 0.5342, compared with 0.6177, the maximum span of the entire known, avian carotenoid plumage gamut. Thus, canthaxanthin pigments in these three species achieve approximately 86 per cent of the maximum span achieved by all carotenoids. Given that the rest of these carotenoid colours set are produced by a wide diversity of molecules, these results show that the effect of carotenoid binding by feather proteins on plumage coloration perceived by birds can be at least as large as the effect on the spectra of the
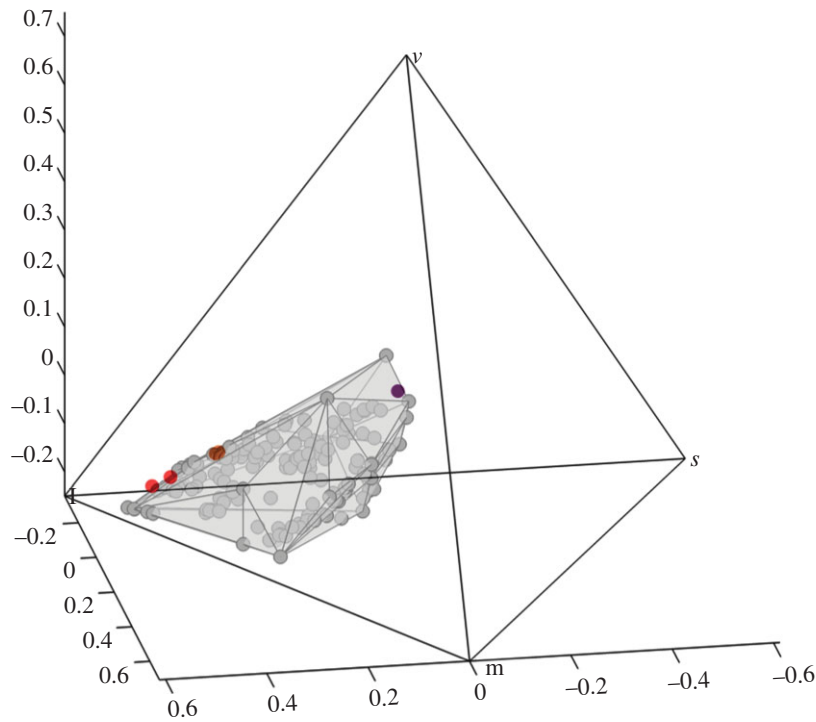
Figure 7. The plumage colours of *E. ruber* (red dots), *P. rubra* (orange dots) and *I. isabellae* (purple dot) modelled in a tetrahedral avian color space. The grey polyhedron represents the total diversity of colour perceptions produced by carotenoid plumages of 145 plumage patches from 52 species in 23 avian families.

Table 1. Frequencies (cm^{-1}) of rR main bands observed in the feathers from *P. rubra*, *E. ruber* and *I. isabellae*.

excitation wavelength (nm)	band	*P. rubra*	*E. ruber*	*I. isabellae*
457.9	ν_1	1514.3	1519.7	n.a.
	ν_2	1157.8	1159.1	n.a.
	ν_3	1007.5	1006.4	n.a.
	ν_4	972.2; 962.2; 952	963.1	n.a.
488	ν_1	1514.3	1514.8	1507.5
	ν_2	1157.8	1157	1155; (1164.7, 1174.5)
	ν_3	1007.5	1004.4	1008.7
	ν_4	972.2; 963.1; 952	963.1	965.5; 953.7
514.5	ν_1	1514.3	1512.8	1508.6
	ν_2	1158.2	1155.3	1156.3; (1165, 1175.7)
	ν_3	1007.2	1003.5	1009.8
	ν_4	972.2; 963.1; 952	961.6	965.5; 954.9
528.7	ν_1	1514.3	1514.1	1508.6
	ν_2	1158.6	1157	1156.3; (1165, 1175.4)
	ν_3	1008.7	1004.4	1009.8
	ν_4	972.2; 963.1; 952	963.1	965.5; 954.9
568.2	ν_1	n.a.	1512.1	1509.6
	ν_2	n.a.	1156.1	1156; (1165, 1176.5)
	ν_3	n.a.	1004.4	1010.4
	ν_4	n.a.	964.6	964.3; 953.8

bound pigments induced by variation in the molecular structure itself.

4. DISCUSSION

HPLC chromatographic analyses, chemical analysis and electronic reflectance and absorption spectroscopy carried out on differently coloured feathers of *P. rubra*, *E. ruber* and *I. isabellae* indicate unambiguously that their colour results from the same

carotenoid pigment, canthaxanthin. We can also eliminate the possibility that the purple coloration is the result of a structural colour. Small-angle X-ray scattering (SAXS) data from Saranathan *et al.* [42] have shown that *I. isabellae* lacks any colour-producing nanostructure, and is indistinguishable from a random heterogeneous mixture of two materials with a well-defined interface (electronic supplementary material, figure S2). Thus, the colour of purple *Iodopleura* feathers is a distinctly pigmentary phenomenon, and is not
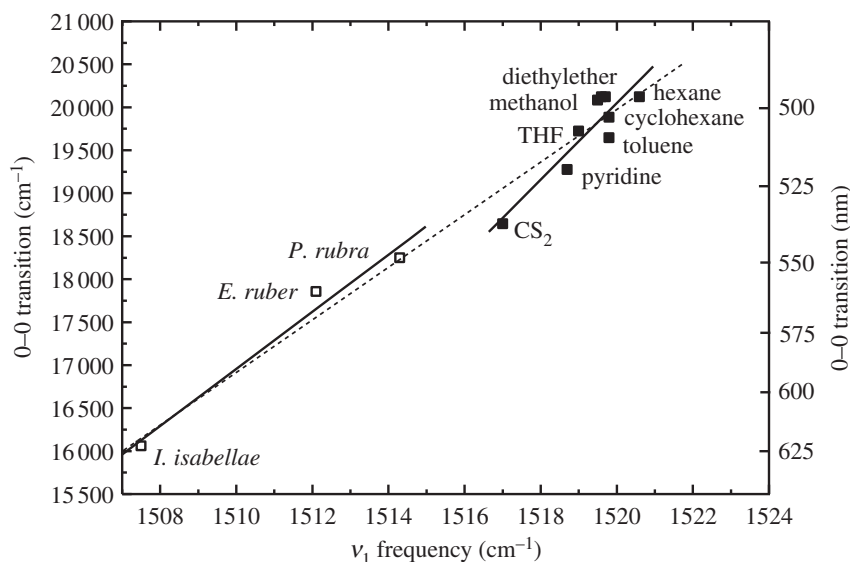
Figure 8. Correlation between the position of the (0–0) spectral origin of the $S_0 \to S_2$ transition and the ν_1 rR band of canthaxanthin in different solvents (solid squares) and in the feathers (open squares) of *P. rubra*, *E. ruber* and *I. isabellae*. All spectra were taken using 514.5 nm excitation. The solid lines represent a fit of the data to two independent linear functions. The dashed line represents a fit of the data to a single line.

the result of interference, or coherent scattering, of blue light wavelengths.

HPLC of extracted carotenoid molecules and the rR spectra of the feathers clearly indicate that canthaxanthin is present in these feathers in an *all-trans* geometric isomeric configuration. Furthermore, in all rR spectra from feathers (figure 6), the ν_4 band exhibits a well-structured lineshape and little variation with the excitation wavelength, indicating that the canthaxanthin molecules in each of the feathers have a single isomeric configuration; i.e. that they are all experiencing the same the out-of-plane distortions along the π-electron conjugated chain. Such distortions are determined by the interactions experienced by the carotenoid upon binding to the protein [20]. Therefore, we can conclude that canthaxanthin in the feathers within each species is not bound in a variable fashion within the protein matrix, but is bound in a highly consistent manner in each species.

However, the binding of canthaxanthin in the different feathers of the three species of birds varies substantially in a manner that is consistent with the observed differences in absorption and feather colour. Specifically, the largest differences among the feather rR spectra were the substantial downshift of the ν_1 band in the purple feathers of *I. isabellae* in comparison with the red feathers of *P. rubra* or *E. ruber*, or to canthaxanthin in solution (figures 5 and 6; table 1). The frequency of the ν_1 band is functionally associated (i.e. correlates with the length of C=C bond conjugation) with the stretching of C=C double bonds [29,32,50]. The effective length of the C=C double bond chain of the carotenoid backbone also has a fundamental impact on the position of the allowed $S_0 \to S_2$ transition, which produces the absorbance spectrum of carotenoid molecules. The effect on the absorption spectra due to differences in the length of the C=C double bond chain of carotenoid molecules is well-documented [46]. These results demonstrate that an extension of the

π-electron C=C double bond chain length of a carotenoid molecule bound to feather protein can substantially affect the absorption of the pigment and the colour produced. As previously mentioned, an X-ray structure analysis of canthaxanthin has revealed that the terminal rings in the molecule are twisted out of the plane of the conjugated double bond chain by approximately 55°, which inhibits π-electron delocalization into the ring structures [53]. Thus, planarization of the terminal rings upon binding to the protein can lead to an extension of the C=C double bond chain length and produce a red-shift in the absorption of the molecule [47]. Thus, the observed increase in the C=C double bond chain length in *I. isabellae* predicts the red-shift in absorption and, contributes to the violet colour produced.

In solution, the position of the electronic absorption spectra of carotenoids depends on the polarizability of the environment (figure 4). We documented this effect by measuring the rR spectrum of canthaxanthin in many different solvents and plotting the ν_1 values on the same graph with those obtained from the feathers (figure 8). The data reveal a correlation between the measured frequency of the ν_1 band of canthaxanthin and the position of its electronic absorption transition, indicating that the electronic structure of the conjugated π-electron system in the ground state of canthaxanthin, which the ν_1 band probes, is sensitive to solvent polarizability. If we make the same correlation between the ν_1 band in feathers and the position of the lowest energy component of their absorption spectra, the slope of line associated with the canthaxanthin feathers is similar to, although slightly shallower than, the slope of the line obtained from canthaxanthin in various solvents and associated with changes in solvent polarizability (solid lines in figure 8).

For carotenoids in solution, a shallower slope of this correlation is predicted when other factors besides polarizability affect the position of the absorption

bands of carotenoid molecules; e.g. differences among solvents that affect the carbon-carbon double bond/single bond order alternation [56,57]. Likewise, the difference in slope between canthaxanthin in solvents and in feathers could reflect additional properties of the binding of canthaxanthin in the feathers. However, it must be noted that it is possible to fit all the data (i.e. from both solvents and feathers) with a single line very close in slope to that determined for the feathers alone (dashed line in figure 8), although canthaxanthin in CS_2 and in pyridine lie substantially off the line fitted to all the data (see the dashed line in figure 8).

The results suggest that the position of the $S_0 \rightarrow S_2$ transition of canthaxanthin could be governed by the local polarizability of the carotenoid environment in the feathers. But, the likelihood of this hypothesis depends on the possibility of substantial variation in the refractive index of the protein binding site among species of birds. The refractive index, n, of the β-keratin matrix in which the carotenoid molecules are embedded is fairly high at 1.58 [58], which corresponds to a polarizability, $R(n)$, value of 0.333, typical of many solids at room temperature. An $R(n)$ value of 0.333 predicts the position of the $S_0 \rightarrow S_2$ transition of keratin-bound canthaxanthin to be around 525 nm (figure 4), which would be blue-shifted by approximately 11 nm compared with that observed for canthaxanthin in CS_2 (figure 2b). Although the exact position of the spectral origin (0–0) band of canthaxanthin in feathers is difficult to assess accurately (figure 2b), the (0–0) energies derived from the feather absorption lineshapes indicate a red-shift when compared with that observed for canthaxanthin in CS_2, (figure 8) and not a blue-shift.

To obtain the observed (0–0) transition value of approximately 16 000 cm^{-1} for canthaxanthin in *I. isabellae* feathers (figure 8) based on polarizability alone would require a value of approximately 0.6 for β-keratin (figure 4), which corresponds to a refractive index of 2.3. That is an extraordinarily large, biologically impossible value that it is equivalent to many metals. Clearly, the data indicate that a change in polarizability alone cannot explain the variation in canthaxanthin absorption among feathers.

The analysis of the ν_4 bands further documents that the precise configuration of canthaxanthin is different between the feathers of different species. Two parameters are important when considering the ν_4 bands: the frequencies of the observed components, which depend on the position of the out-of-plane distortion in the molecule, and their intensity, which depends on the extent of the out-of plane distortion. In *P. rubra* feathers, the ν_4 band is slightly more intense compared with that of canthaxanthin in solvents, and about one-fourth of that of the ν_3 band. This indicates that the binding of canthaxanthin to the feather protein induces a small, additional distortion of the π-electron conjugated chain that is not present in organic solvents. In *E. ruber,* the ν_4 band is nearly twice as intense as in *P. rubra*. Thus, carotenoid binding in *E. ruber* induces the same additional distortion to the molecule as in *P. rubra* but with a greater magnitude. Finally, in *I. isabellae*, the intensity of the ν_4 band reaches that of the ν_3 band, with two main components between

953.7 and 965.5 cm^{-1} (table 1). These frequencies are only slightly higher than the corresponding ν_4 band frequencies observed for *P. rubra* and *E. ruber* feathers. From this, we can conclude that the binding sites provided by the three feathers induce out-of-plane distortions of canthaxanthin around carbon–carbon single bonds of varying magnitudes, and that the most substantial distortion of canthaxanthin is observed in *I. isabellae* feathers. It is interesting to note that the more distorted canthaxanthin becomes compared with its structure in solvents, the redder the absorption of the feathers.

Variation in the position and width of ν_1 band were observed with different excitation wavelengths in each of the three species. In *P. rubra,* variation in the ν_1 band with excitation wavelength was limited to a change in the fwhm of the peak. By contrast, in the feathers from *E. ruber* and *I. isabellae*, the ν_1 band shifted noticeably in frequency with excitation wavelength. More specifically, for *P. rubra* feathers, where only an increase in the width of the ν_1 rR band is observed, the absorption spectrum is broader when compared with that of canthaxanthin in solution. *Eudocimus ruber* feathers, for which ν_1 frequencies varied between 1512.1 and 1519.7 cm^{-1} (approx. 7.5 cm^{-1}) with excitation wavelength, exhibit an even broader absorption band (table 1). The range of ν_1 frequencies observed bracket the ν_1 peak of *P. rubra* (1514.3 cm^{-1}), and their absorption spectrum also extends beyond both ends of that observed from *P. rubra*. Finally, for *I. isabellae*, the ν_1 frequency varies between 1507.5 and 1509.6 cm^{-1} (approx. 2 cm^{-1}) depending on the excitation wavelength. This result correlates with a narrower absorption spectra for *I. isabellae* than observed in *E. ruber*.

Planarization of the terminal rings of canthaxanthin will extend the π-electron conjugation farther along the carbon chain. Lengthening the extent of π-electron conjugation is known to down-shift the rR ν_1 band and red-shift the absorption spectrum of carotenoids [32,59]. However, rR studies on carotenoids and polyenes having different π-electron conjugated chain lengths show that on average, there is approximately 15 nm of a red-shift in the absorption spectrum and approximately 6 cm^{-1} of a down-shift in the rR ν_1 band position for every added double bond [29,59]. Thus, the approximately 6–7 cm^{-1} down-shift in the ν_1 band observed in the feathers of *I. isabellae* compared with *P. rubra* (table 1) is not enough to account for all of the approximately 75 nm red-shift occurring between their absorption spectra (figure 8). Moreover, comparing the ν_1 band of canthaxanthin in hexane (1520.5 cm^{-1}) with that of the pigment in *I. isabellae* feathers (1508.6 cm^{-1}), both recorded using 514.5 nm excitation, shows a difference of 11.9 cm^{-1}. This would only amount to a difference of 11.9 cm^{-1} × (15 nm/6 cm^{-1}) ≈ 30 nm between these two samples, which is clearly not enough to account for the violet purple colour of *I. isabellae* feathers.

An additional factor that can influence carotenoid pigment absorption is the formation of molecular aggregates. Absorption and rR spectroscopic investigations of crystalline and aggregated samples of several *all-trans*-

carotenoids [51,60,61] described the effect of close proximity of the pigments on their spectral properties. The data reveal that carotenoids packed in a head-to-tail arrangement, called J-aggregates in the molecular exciton coupling theory [62], undergo a significant red-shift in their absorption spectra. This is because absorption into an energetically low-lying exciton state, formed when π-electron conjugated molecules are brought into close proximity, is red-shifted relative to the absorption bands associated with monomeric, unaggregated molecules. In fact, canthaxanthin undergoes a significant red-shift from 495 nm (20 202 cm^{-1}) in solution (monomeric) to 581 nm (17 202 cm^{-1}) in J-aggregate crystalline form [60]. Salares *et al.* [51] reported a 5 cm^{-1} downshift of the ν_1 band of canthaxanthin, from 1523 cm^{-1} in acetone to 1518 cm^{-1} for the aggregated molecule in 10 per cent acetone–H$_2$O solution. Monomeric canthaxanthin in the eight different solvents used here has ν_1 values that span the 1520.5–1517 cm^{-1} range (using 514.5 nm excitation), and *I. isabellae* feathers have its ν_1 band at 1508.6 cm^{-1} (using the same excitation λ). This corresponds to an approximately 10 cm^{-1} downshift, roughly twice that reported by Salares *et al.* [51] for carotenoid aggregates. This strongly suggests that carotenoid aggregation in the feathers is not the sole source of the spectral shift, but it appears to be an important factor, in addition to protein binding, needed to produce the violet colour of *I. isabellae*. It is not difficult to envision that canthaxanthin may be taken up into the keratin protein fibres of feathers in a head-to-tail manner so that it forms J-aggregates or related aggregated species, which could themselves be sensitive to the properties of the local environment provided by keratin. However, additional work will be required to confirm whether carotenoid are bound directly to β-keratin or to another protein or molecule, and whether molecular aggregates of canthaxanthin are present in the feathers of *I. isabellae* and other bird species as well.

5. CONCLUSIONS

These results confirm that different species of birds have evolved differences in the carotenoid binding to feather keratin proteins. Our findings support the following conclusions:

— Different canthaxanthin binding modes among the three different species examined produces changes in feather reflectance spectrum that are perceived by birds as strikingly different colours. The effect of protein binding on plumage coloration can be at least as significant on plumage colour as changes in molecular structure.

— Canthaxanthin is bound in a consistent manner by feather proteins in each of the feathers from the three species analysed, but each species induces a different degree of C=C double bond extension (ν_1) and out-of-plane twists of the carbon backbone (ν_4) of the bound pigment.

— Different subpopulations of all *trans*-canthaxanthin molecules are present in each of the feathers, which may be distinguished on the basis of their rR

properties, particularly the frequency of their ν_1 band. These changes do not affect the general *all-trans* geometric structure of canthaxanthin, but qualitatively correlate with the width of the absorption of each of the feathers.

— The degree of canthaxanthin distortion, especially the C=C double bond extension revealed through ν_1, correlates well with the red-shift in the absorption spectra exhibited by canthaxanthin in each of the three feathers studied. However, the entire extent of the red-shift cannot be explained by the refractive index/polarizability of the molecular environment nor by planarization of the canthaxanthin terminal rings alone, although those are contributing factors. Very likely, linear, end-to-end molecular aggregation of the carotenoid pigments is an additional important factor.

REFERENCES

1 Blount, J. D. & McGraw, K. J. 2008 Signal functions of carotenoid colouration. In *Carotenoids volume 4: nutrition and health* (eds G. Britton, S. Liaaen-Jensen & H. Pfander), pp. 213–232. Basel, Switzerland; Boston, MA; Berlin, Germany: Birkhäuser.

2 McGraw, K. J. 2006 Mechanics of carotenoid-based coloration. In *Bird coloration volume 1: mechanisms and measurements* (eds G. E. Hill & K. J. McGraw), pp. 177–242. Cambridge, MA: Harvard University Press.

3 Stoddard, M. C. & Prum, R. O. 2011 How colorful are birds? Evolution of the avian plumage color gamut. *Behav. Ecol.* **22**, 1042–1052. (doi:10.1093/beheco/arr088)

4 Hill, G. E. & McGraw, K. J. (eds). 2006 *Bird coloration, volume 1: mechanisms and measurements.* Cambridge, MA: Harvard University Press.

5 Hill, G. E. & McGraw, K. J. (eds). 2006 *Bird coloration, volume 2: function and evolution.* Cambridge, MA: Harvard University Press.

6 Prum, R. O. 2006 Anatomy, physics, and evolution of avaian structural colors. In *Bird coloration volume 1: mechanisms and measurements* (eds G. E. Hill & K. J. McGraw), pp. 295–353. Cambridge, MA: Harvard University Press.

7 McGraw, K. J. 2006 Mechanics of melanin-based coloration. In *Bird coloration volume 1: mechanisms and*

measurements (eds G. E. Hill & K. J. McGraw), pp. 243–294. Cambridge, MA: Harvard University Press.

8 Prum, R. O., Torres, R. H., Williamson, S. & Dyck, J. 1998 Coherent light scattering by blue feather barbs. *Nature* **396**, 28–29. (doi:10.1038/23838)

9 McGraw, K. J. 2003 Melanins, metals, and mate quality. *Oikos* **102**, 402–406. (doi:10.1034/j.1600-0579.2003.12513.x)

10 Shawkey, M. D. & Hill, G. E. 2005 Carotenoids need structural colours to shine. *Biol. Lett.* **1**, 121–124. (doi:10.1098/rsbl.2004.0289)

11 Stradi, R., Celentano, G., Rossi, E., Rovati, G. & Pastore, M. 1995 Carotenoids in bird plumage: the carotenoid pattern in a series of Paleartic Carduelinae. *Comp. Biochem. Physiol.* **110B**, 131–143.

12 Goodwin, T. W. 1984 *The biochemistry of carotenoids. Volume II. Animals.* London, UK: Chapman Hall.

13 Schiedt, K. 1998 Absorption and metabolism of carotenoids in birds, fish and crustaceans. In *Carotenoids volume 3: biosynthesis and metabolism* (eds G. Britton, S. Liaaen-Jensen & H. Pfander), pp. 285–358. Basel, Switzerland; Boston, MA; Berlin, Germany: Birkhäuser.

14 Brush, A. H. & Power, D. M. 1976 House finch pigmentation—carotenoid metabolism and effect of diet. *Auk* **93**, 725–739.

15 McGraw, K. J., Hill, G. E., Stradi, R. & Parker, R. S. 2001 The influence of carotenoid acquisition and utilization on the maintenance of species-typical plumage pigmentation in the male American goldfinches (*Carduelis tristis*) and northern cardinal (*Cadinalis cardinalis*). *Physiol. Biochem. Zool.* **74**, 843–852. (doi:10.1086/323797)

16 Stradi, R., Rossi, E., Celentano, G. & Bellardi, B. 1996 Carotenoids in bird plumage: the pattern in three *Loxia* species and in *Pinicola enucleator*. *Comp. Biochem. Physiol.* **113B**, 427–432.

17 McGraw, K. J., Hill, G. E. & Parker, R. S. 2005 The physiological costs of being colorful: nutritional control of carotenoid utilization in the American goldfinch, *Carduelis tristis. Anim. Behav.* **69**, 653–660. (doi:10.1016/j.anbehav.2004.05.018)

18 McGraw, K. J., Hill, G. E. & Parker, R. S. 2003 Carotenoid pigments in a mutant cardinal: Implications for the genetic and enzymatic control mechanisms of carotenoid metabolism in birds. *Condor* **105**, 587–592. (doi:10.1650/7281)

19 Hudon, J. & Brush, A. 1992 Identification of carotenoid pigments in birds. In *Carotenoids part a: chemistry, separation, quantitation, and antioxidation* (ed. L. Packer), pp. 312–321. San Diego, CA: Academic Press.

20 Britton, G. & Helliwell, J. R. 2008 Carotenoid–protein interactions. In *Carotenoids volume 4: nutrition and health* (eds G. Britton, S. Liaaen-Jensen & H. Pfander), pp. 99–117. Basel–Boston–Berlin, Germany: Birkhäuser.

21 Brush, A. H. 1972 Correlation of protein electrophoretic pattern with morphology of normal and mutant feathers. *Biochem. Genet.* **7**, 87–93. (doi:10.1007/BF00487012)

22 Brush, A. H. 1986 Tissue specific protein heterogeneity in keratin structures. *Biochem. Syst. Ecol.* **14**, 547–551. (doi:10.1016/0305-1978(86)90016-5)

23 Weesie, R. J., Jansen, F. J. H. M., Merlin, J. C., Lugtenburg, J., Britton, G. & de Groot, H. J. M. 1997 13C Magic angle spinning NMR analysis and quantum chemical modeling of the bathochromic shift of astaxanthin in α-Crustacyanin, the blue carotenoprotein complex in the carapace of the lobster *Homarus gammarus. Biochemistry* **36**, 7288–7296. (doi:10.1021/bi9631982)

24 Britton, G. *et al.* 1997 Carotenoid blues: structural studies on carotenoproteins. *Pure Appl. Chem.* **69**, 2075–2084. (doi:10.1351/pac199769102075)

25 Cianci, M., Rizkallah, P. J., Olczak, A., Raftery, J., Chayen, N. E., Zagalsky, P. F. & Helliwell, J. R. 2002 The molecular basis of the coloration mechanism in lobster shell: β-crustacyanin at 3.2-Å resolution. *Proc. Natl Acad. Sci. USA* **99**, 9795–9800. (doi:10.1073/pnas.152088999)

26 Ilagan, R. P., Christensen, R. L., Chapp, T. W., Gibson, G. N., Pascher, T., Polivka, T. & Frank, H. A. 2005 Femtosecond time-resolved absorption spectroscopy of astaxanthin in solution and in α-crustacyanin. *J. Phys. Chem. A* **109**, 3120–3127. (doi:10.1021/jp0444161)

27 Veronelli, M., Zerbi, G. & Stradi, R. 1995 *In situ* resonance Raman spectra of carotenoids in birds feathers. *J. Raman Spectrosc.* **26**, 683–692. (doi:10.1002/jrs.1250260815)

28 Robert, B., Horton, P., Pascal, A. A. & Ruban, A. V. 2004 Insights into the molecular dynamics of plant light-harvesting proteins *in vivo. Trends Plant Sci.* **9**, 1360–1385. (doi:10.1016/j.tplants.2004.06.006)

29 Koyama, Y. 1995 Resonance Raman spectroscopy. In *Carotenoids volume 1B: spectroscopy* (eds G. Britton, S. Liaaen-Jensen & H. Pfander), pp. 135–146. Basel, Switzerland; Boston, MA; Berlin, Germany: Birkhäuser.

30 Robert, B. 1999 The electronic structure, stereochemistry and resonance Raman spectroscopy of carotenoids. In *Advances in photosynthesis* (eds H. A. Frank, A. J. Young & G. Britton & R. J. Cogdell), pp. 189–201. Dordrecht, The Netherlands; Boston, MA; London, UK: Kluwer Academic Publishers.

31 Ruban, A. V., Pascal, A. A., Robert, B. & Horton, P. 2001 Configuration and dynamics of xanthophylls in light-harvesting antennae of higher plants: spectroscopic analysis of isolated light-harvesting complex of photosystem II and thylakoid membranes. *J. Biol. Chem.* **276**, 24 862–24 870.

32 Robert, B. 2009 Resonance Raman spectroscopy. *Photosynth. Res.* **101**, 147–155. (doi:10.1007/s11120-009-9440-4)

33 Fox, D. L. & Hopkins, T. S. 1966 Carotenoid fractionation in the scarlet ibis. *Comp. Biochem. Physiol.* **19**, 267–278. (doi:10.1016/0010-406X(66)90565-2)

34 Fox, D. L. 1962 Carotenoids of the Scarlet Ibis. *Comp. Biochem. Physiol.* **5**, 31–43. (doi:10.1016/0010-406X(62)90139-1)

35 Hudon, J. 1990 Unusual carotenoid use by the western tanager (*Piranga ludoviciana*) and its evolutionary implications. *Can. J. Zool.* **69**, 2311–2320. (doi:10.1139/z91-325)

36 LaFountain, A. M., Kaligotla, S., Cawley, S., Riedl, K. M., Schwartz, S. J., Frank, H. A. & Prum, R. O. 2010 Novel methoxy-carotenoids from the burgundy-colored plumage of the pompadour cotinga *Xipholena punicea. Arch. Biochem. Biophys.* **504**, 142–153. (doi:10.1016/j.abb.2010.08.006)

37 Stoddard, M. C. & Prum, R. O. 2008 Evolution of avian plumage color in a tetrahedral color space: a phylogenetic analysis of new world buntings. *Am. Nat.* **171**, 755–776. (doi:10.1086/587526)

38 Endler, J. A. & Mielke, P. W. 2005 Comparing entire colour patterns as birds see them. *Biol. J. Linn. Soc.* **86**, 405–431. (doi:10.1111/j.1095-8312.2005.00540.x)

39 Ödeen, A. & Håstad, O. 2003 Complex distribution of avian color vision systems revealed by sequencing the SWS1 opsin from total DNA. *Mol. Biol. Evol.* **20**, 855–861. (doi:10.1093/molbev/msg108)

40 Carvalho, L. S., Cowing, J. A., Wilkie, S. E., Bowmaker, J. K. & Hunt, D. M. 2007 The molecular evolution of avian ultraviolet- and violet-sensitive visual pigments. *Mol. Biol. Evol.* **24**, 1843–1852. (doi:10.1093/molbev/msm109)

41 Britton, G., Liaaen-Jensen, S. & Pfander, H. 2004 *Carotenoids handbook.* Basel, Switzerland; Boston, MA; Berlin, Germany: Birkhäuser.

42 Saranathan, V., Forster, J. D., Noh, H., Liew, S. F., Mochrie, S. G. J., Cao, H., Dufresne, E. R. & Prum, R. O. In press. Structure and optical function of amorphous photonic nanostructures from avian feather barbs: a comparative small angle X-ray scattering (SAXS) analysis of 229 bird species. *J. R. Soc. Interface.*

43 Noh, H., Liew, S. F., Saranathan, V., Prum, R. O., Mochrie, S. G. J., Dufrense, E. R. & Cao, H. 2010 Double scattering of light from biophotonic nanostructures with short-range order. *Opt. Expr.* **18**, 11 942–11 948. (doi:10.1364/OE.18.011942)

44 Noh, H., Liew, S. F., Saranathan, V., Mochrie, S. G. J., Prum, R. O., Dufrense, E. R. & Cao, H. 2010 How noniridescent colors are generated by quasi-ordered structures of bird feathers. *Adv. Mater.* **22**, 2871–2880. (doi:10.1002/adma.200903699)

45 Glatter, O. & Kratky, O. 1983 *Small angle X-ray scattering*, 2nd edn. London, UK: Academic Press.

46 Isler, O. 1971 *Carotenoids*. Basel, Switzerland: Birkhäuser.

47 Bartalucci, G., Coppin, J., Fisher, S., Hall, G., Helliwell, J. R., Helliwell, M. & Liaaen, J. S. 2007 Unravelling the chemical basis of the bathochromic shift in the lobster carapace; new crystal structures of unbound astaxanthin, canthaxanthin, and zeaxanthin. *Acta Crystallogr. Sect. B: Struct. Sci.* **B63**, 328–337. (doi:10.1107/S0108768106052633)

48 Polívka, T. & Frank, H. A. 2010 Molecular factors controlling photosynthetic light harvesting by carotenoids. *Acc. Chem. Res.* **43**, 1125–1134. (doi:10.1021/ar100030m)

49 Renge, I. & Sild, E. 2011 Absorption shifts in carotenoids-influence of index of refraction and submolecular electric fields. *J. Photochem. Photobiol. A* **218**, 156–161. (doi:10.1016/j.jphotochem.2010.12.015)

50 Koyama, Y., Kito, M., Takii, T., Saiki, K., Tsukida, K. & Yamashita, J. 1982 Configuration of the carotenoid in the reaction centers of photosynthetic bacteria. Comparison of the resonance Raman spectrum of the reaction centers of *Rhodopseudomonas sphaeroides* G1C with those of cis-trans isomers of ß-carotene. *Biochim. Biophys. Acta* **680**, 109–118. (doi:10.1016/0005-2728(82)90001-9)

51 Salares, V. R., Young, N. M., Carey, P. R. & Bernstein, H. J. 1977 Excited state (exciton) interactions in polyene aggregates. *J. Raman Spectrosc.* **6**, 282–288. (doi:10.1002/jrs.1250060605)

52 Lutz, M., Szponarski, W., Berger, G., Robert, B. & Neumann, J.-M. 1987 The stereoisomerization of bacterial,

reaction-center-bound carotenoids revisited: an electronic absorption, resonance Raman and NMR study. *Biochim. Biophys. Acta* **894**, 423–433. (doi:10.1016/0005-2728(87)90121-6)

53 Bart, J. C. J. & MacGillavry, C. H. 1968 The crystal and molecular structure of canthaxanthin. *Acta Crystallogr. Sect. B* **24**, 1587–1606. (doi:10.1107/S056774086800470X)

54 Ruban, A. V., Horton, P. & Robert, B. 1995 Resonance Raman spectroscopy of the photosystem II light-harvesting complex of green plants: a comparison of trimeric and aggregated states. *Biochem* **34**, 2333–2337. (doi:10.1021/bi00007a029)

55 Cuthill, I. C. 2006 Color perception. In *Bird coloration, volume 1: mechanisms and measurements* (eds G. E. Hill & K. J. McGraw), pp. 3–40. Cambridge, MA: Harvard University Press.

56 Araki, G. & Murai, T. 1952 Molecular structure and absorption spectra of carotenoids. *Prog. Theor. Phys.* **8**, 639–654. (doi:10.1143/PTP.8.639)

57 Angerhofer, A., Bornhauser, F., Gall, A. & Cogdell, R. J. 1995 Optical and optically detected magnetic-resonance investigation on purple photosynthetic bacterial antenna complexes. *Chem. Phys.* **194**, 259–274. (doi:10.1016/0301-0104(95)00022-G)

58 Brink, D. J. & van der Berg, N. G. 2004 Structural colours from the feathers of the bird *Bostrychia hagedash*. *J. Phys. D: Appl. Phys.* **37**, 813–818. (doi:10.1088/0022-3727/37/5/025)

59 Koyama, Y. & Fujii, R. 1999 Cis-trans carotenoids in photosynthesis: configurations, excited-state properties and physiological functions. In *The photochemistry of carotenoids* (eds H. A. Frank, A. J. Young, G. Britton & R. J. Cogdell), pp. 161–188. Dordrecht, The Netherlands: Kluwer Academic Publishers.

60 Mori, Y. 2001 Introductory studies on the growth and characterization of carotenoid solids: an approach to carotenoid solid engineering. *J. Raman Spectrosc.* **32**, 543–550. (doi:10.1002/jrs.715)

61 Gruszecki, W. I. 1991 Structural characterization of the aggregated forms of violaxanthin. *J. Biol. Phys.* **18**, 99–109. (doi:10.1007/BF00395057)

62 Gaier, K., Angerhofer, A. & Wolf, H. C. 1991 The lowest excited electronic singlet states of all-trans β-carotene single crystals. *Chem. Phys. Lett.* **187**, 103–109. (doi:10.1016/0009-2614(91)90492-R)